

# Novel least-mean-square-based adaptive estimator for unknown periodic disturbances

Pan Yu<sup>1</sup>, Chen Xu<sup>1</sup>, and Jinhua She<sup>2</sup>

<sup>1</sup> School of Information Science and Technology and Beijing Institute of Artificial Intelligence, Beijing University of Technology, Beijing 100124, China

panyu@bjut.edu.cn

chenxu@emails.bjut.edu.cn

<sup>2</sup> School of Engineering, Tokyo University of Technology, Hachioji 192-0982, Japan  
she@bs.teu.ac.jp

**Abstract.** Unknown periodic disturbances are widely found in practical control engineering. A least-mean-square-based adaptive estimator (LMS-AE) is developed to cope with this kind of disturbances. Enlightened by the LMS adaptive filter, an LMS-AE is devised to iteratively learn the amplitude and phase of the components of the periodic disturbances, after the frequency characteristics are extracted by a data-driven technique. Then, the output error between the real system and the observer is introduced supervise the learning process of the pending weights by the LMS algorithm. Moreover, the convergence condition of the weight updated law is given. The stability conditions of the LMS-AE-based closed-loop control system are analyzed by the separation theorem. The effectiveness and superiority of this proposed control method are verified by a case study and comparisons with other methods.

**Keywords:** Adaptive disturbance estimator · Least mean square (LMS)  
· Equivalent input disturbance (EID) · Fourier series.

## 1 Introduction

Periodic repetitive motions are widely found in automatic control systems. Although these systems are capable of high precision and long time operation, such as rotary machines, and elastic robots [1, 2], the simultaneous repetitive motions can also introduce periodic disturbances. Moreover, these disturbances not only have an impact on the performance of the system, but also destabilise the system [3].

For periodic disturbances, they are generally equivalent to a combination of fundamental and harmonics waves, so how to use the frequency information of the components of the disturbances for rejection is the most critical issue. Disturbance observer-based control (DOBC) is a widely used method for estimating and compensating for disturbances. Based on the DOBC, in [4] the periodic observer (PDOB) which uses an adaptive notch filter to estimate the fundamental frequency of the periodic disturbance, then compensates the periodic disturbance. State observer is another useful tool for disturbances rejection.

Not only that, many periodic disturbances rejection methods incorporate adaptive approaches. In [5] a lumped disturbance is estimated by the DOB for the initial time period and stored in memory storages, then update the information of the disturbances for each time period by the periodic adaptation law. And for eliminating the frequency-varying periodic disturbance, an adaptive periodic-disturbance observer (APDOB) was proposed [6].

However, the DOBC method requires an accurate model of disturbances. The disturbance rejection performance of the DOBC method is not satisfactory when perturbations are present in the disturbance model [7]. So many applications are limited due to this. The equivalent-input-disturbance (EID) method was developed to eliminate this limitation [8]. In [9], She and Kou compared the DOBC method with the EID approach. The result showed that the EID method is more practical than the DOBC method because the latter assumes the presence of equivalent input disturbance and it is easier to tune the disturbance-rejection performance. The EID method equivalently compensates for the disturbance in the input channels of the system, ultimately reject the effects of the disturbance at the output of the system. This method is effective for both matched and unmatched interference. Additionally, it simplifies the configuration of the estimator by eliminating the need for a disturbance model, inverse dynamics of plant, and input matrix of disturbances. The effectiveness of the EID method has been demonstrated in numerous systems [10–12].

The adaptive algorithms were derived using the filtering method and optimal prediction to solve the Wiener-Hoff equation [13]. The least-mean-square (LMS) adaptive filter (LMS-AF), is a formal method in processing signals containing noise [14]. By updating the weight against the error gradient, the principle of the algorithm is to minimize the error between output and expectation.

Among the above methods, although LMS-AF is a standard filtering adaptive algorithm, it can only have pretty good effect on some signals including Gaussian noise due to the limitation of the input. The EID method can suppress most of the noises well, but due to the structure, it has a weak effect on the mismatched high-frequency disturbances. This makes us design the LMS-based adaptive estimator (LMS-AE), a disturbance rejection estimator that combines the advantages of both methods.

## 2 SYSTEM CONFIGURATION

The configuration of the developed LMS-AE-based system is shown in Fig. 1. It has five parts: a plant, a Luenberger observer, an LMS-AE, a state feedback controller, and an internal model.

Consider the following discrete system with a disturbance

$$\begin{cases} x(k+1) = Ax(k) + Bu(k) + B_d d(k) \\ y(k) = Cx(k) \end{cases} \quad (1)$$

where  $x(k) \in \mathbb{R}^{n_x}$  is the state; and  $u(k) \in \mathbb{R}^{n_u}$ ,  $y(k) \in \mathbb{R}^{n_y}$ , and  $d(k) \in \mathbb{R}^{n_d}$  are the input, output, and the disturbance, respectively; and  $A$ ,  $B$ , and  $C$  are real constant matrices, and  $B_d$  is the unknown input matrix of the disturbance.

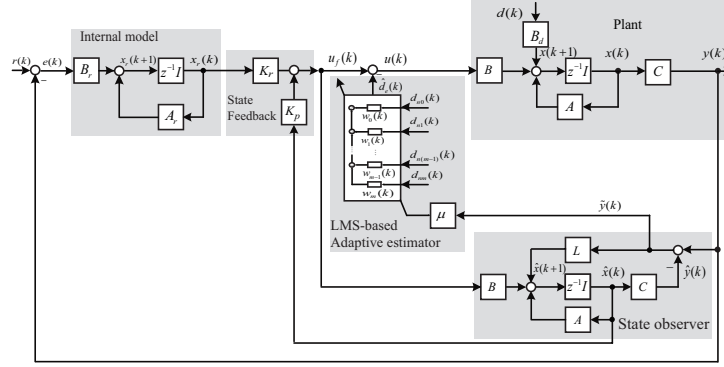


**Fig. 1.** Structure of LMS-AE-based disturbance rejection control system

The following assumptions are made for system design.

**Assumption 1** The nominal plant  $(A, B, C)$  is controllable and observable.

**Assumption 2** The unknown periodic disturbance  $d(k)$  satisfies

$$\|d(k)\| \leq d_m \quad (2)$$

where  $\|d(k)\|$  is the 2-norm of  $d(k)$ ,  $d_m$  is an unknown positive number.

*Remark 1.* Assumption 1 is standard for system design [18] and Assumption 2 usually holds in practice.

A Luenberger observer is used to obtain the state estimate of the system

$$\begin{cases} \hat{x}(k+1) = A\hat{x}(k) + Bu_f(k) + L[y(k) - \hat{y}(k)] \\ \hat{y}(k) = C\hat{x}(k) \end{cases} \quad (3)$$

where  $\hat{x}(k)$ ,  $u_f(k)$ ,  $\hat{y}(k)$ , and  $L$  denote the state, the input, the output, and the gain of the observer respectively.

Denote  $\hat{d}_e(k)$  as the output of the LMS-AE, and incorporating it gives the following new control law

$$u(k) = u_f(k) - \hat{d}_e(k) \quad (4)$$

where  $u_f(k)$  is the original feedback control law.

To ensure the tracking performance of the system, it can be assumed that the internal model of the reference input  $r(k)$  is

$$x_r(k+1) = A_r x_r(k) + B_r [r(k) - y(k)] \quad (5)$$

where  $x_r(k)$  is the state of the internal model, and  $A_r$  and  $B_r$  are constant matrices of suitable dimensions.

Based on the state  $\hat{x}(k)$  of the observer, the original feedback control law is taken as

$$u_f(k) = K_p \hat{x}(k) + K_r x_r(k) \quad (6)$$

where  $K_p$  and  $K_r$  are the control gain.

### 3 LMS-based Adaptive Estimator

Due to the unknown of the disturbances, a data-driven technique is used to extract the characteristics of the external disturbance by the dynamics(3). Using the obtained bases, the LMS-AE is devised to learn the corresponding phases together with the amplitudes.

Define

$$\tilde{x}(k) = x(k) - \hat{x}(k), \quad \tilde{y}(k) = y(k) - \hat{y}(k). \quad (7)$$

Let

$$A_L = A - LC. \quad (8)$$

According to (1), (3), (4), (7), and (8), we obtain error state system

$$\begin{cases} \tilde{x}(k+1) = A_L \tilde{x}(k) - B \hat{d}_e(k) + B_d d(k) \\ \tilde{y}(k) = C \tilde{x}(k), \end{cases} \quad (9)$$

Since  $\tilde{y}$  in (9) represents the error between the output of real and nominal system. It contains the effect of disturbance on the system so the characteristics of the external disturbance can be extracted from  $\tilde{y}$ . And  $\tilde{y}$ , which reflects the performance of disturbance rejection for system, is only affected by disturbance  $d$  and EID estimate  $\hat{d}_e$ , so a threshold  $T_h$  set for  $\tilde{y}$  that extraction only happens when the absolute value of  $\tilde{y}$  is bigger than  $T_h$ .

#### 3.1 Frequency Extraction of Unknown Disturbances

By the Fourier series expansion, a periodic disturbance  $d(t)$  is decomposed as

$$d(t) = \sum_{i=1}^{\infty} d_i(t) = A_0 + \sum_{i=1}^{\infty} A_i \sin(2\pi f_i t + \varphi_i) \quad (10)$$

where  $A_0$  is the DC component,  $A_i$  are the amplitudes,  $f_i$  are the frequencies, and  $\varphi_i$  are the phases.

According to error state system (9), the frequency spectrum of the unknown disturbances can be extracted from  $\tilde{y}$  after the transient state fading away. Therefore, some data-driven methods can be used to conduct the frequency spectrum analysis and obtain  $f_i$  using  $\tilde{y}$  by fast Fourier transform (FFT) method when the observer is designed to be stable.

#### 3.2 LMS-based Learning algorithm

The LMS algorithm is an adaptive algorithm using instantaneous gradient. The LMS-AF is a lateral filter based on the LMS algorithm, of which the inputs are related to current and past values of  $c(k)$ . Denote the input of the LMS-AF  $c_i(k) = c(k - i + 1)$ , ( $i = 1, 2, \dots, n$ ) where  $n$  is the filter dimension and  $k$  is the sample number. By iteration along the direction of the LMS instantaneous gradient, the pending weights  $w_i^c(k)$  are able to approach the optimal weights.

The updated law of the pending weights of the LMS-AF is

$$w_i^c(k+1) = w_i^c(k) + \mu^c c_i(k) e(k) \quad (11)$$

where  $\mu^c$  is fixed related to the input,  $e(k) = y_d(k) - y(k)$  is the error at the  $k$ -th step, and  $y_d(k)$  and  $y(k)$  are the reference and real output of the filter. The convergence condition for the weight is given by

$$0 < \mu^c < \frac{2}{\lambda_{\max}^c} \quad (12)$$

where  $\lambda_{\max}^c$  is the maximum eigenvalue of correlation matrix of the  $\bar{c}(k)$  [14], and  $\bar{c} = [c_0, c_1, \dots, c_n]^T$ .

### 3.3 Adaptive Estimator for Disturbance Rejection

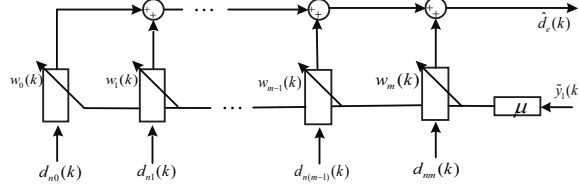


**Fig. 2.** Structure of LMS-AE.

The developed LMS-based adaptive estimator is shown in Fig. 2, where  $d_{ni}(k)$  ( $i = 0, 1, \dots, m$ ) are the input of the LMS-AE including the fundamental and harmonic signal sequences from the frequency characteristics extraction, which replace the sequence of current and past values, and  $w_i(k)$  are the pending weights of  $d_{ni}(k)$ , which are computed by the LMS algorithm. The error of output  $\tilde{y}(k)$  replaces the error of LMS-AF. What LMS-AE does is actually to learn the amplitude and phase of these sinusoidal components.

The output of LMS-AE is summing by multiplying weights and inputs:

$$\hat{d}_e(k) = \sum_{i=0}^m w_i(k) d_{ni}(k) \quad (13)$$

where  $\hat{d}_e(k)$  is an estimate of  $d_e(k)$ .

Similarly, the updated law of weights in LMS-AE are given by

$$w_i(k+1) = w_i(k) + \mu d_{ni}(k) \tilde{y}(k). \quad (14)$$

Accordingly, the convergence condition for the weights are

$$0 < \mu < \frac{2}{\lambda_{\max}^{d_n}} \quad (15)$$

where  $\mu$  is fixed related to the input,  $\lambda_{\max}^{d_n}$  is the maximum eigenvalue of the correlation matrix of  $d_n(k)$  [14], and  $d_n = [d_{n0}, d_{n1}, \dots, d_{nm}]^T$ .

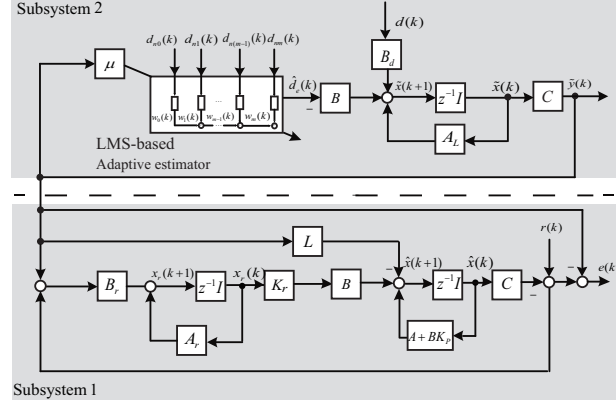


Fig. 3. Equivalent structure of Fig. 1

## 4 Analysis and Design of Control System

The LMS-AE-based control system is analyzed by dividing it into Subsystem 1 and Subsystem 2, as shown in Fig. 3. If both subsystems are stable, so does the entire closed-loop control system in Fig. 1.

### 4.1 Analysis and Design of Subsystem 1

For Subsystem 1, it consists of a Luenberger observer, an internal model, and a state feedback controller.

Define

$$\bar{x}(k) = [\hat{x}(k)^T, x_r(k)^T]^T. \quad (16)$$

Combining (1), (3), (4), (5), and (6), the state-space representation of Subsystem 1 is

$$\begin{cases} \bar{x}(k+1) = \bar{A}\bar{x}(k) + \bar{B}_L\tilde{y}(k) + \bar{B}_r r(k) \\ \tilde{y}(k) = \bar{C}\bar{x}(k) + \tilde{y}(k) \end{cases} \quad (17)$$

where

$$\begin{cases} \bar{A} = \bar{A}_0 + \bar{B}\bar{K}, & \bar{A}_0 = \begin{bmatrix} A & 0 \\ -B_r C & A_r \end{bmatrix}, & \bar{B} = \begin{bmatrix} B \\ 0 \end{bmatrix}, & \bar{K} = [K_p \ K_r] \\ \bar{B}_L = \begin{bmatrix} L \\ -B_r \end{bmatrix}, & \bar{B}_r = \begin{bmatrix} 0 \\ B_r \end{bmatrix}, & \bar{C} = [C \ 0]. \end{cases} \quad (18)$$

Further, we have the following result about the stability.

**Theorem 1.** For bounded  $\tilde{y}(k)$  and  $r(k)$ , if  $\bar{A}$  of (17) is stable, then Subsystem 1 is stable.

#### 4.2 Analysis and Design of Subsystem 2

For Subsystem 2 in Fig. 3, it consists of an error state system (9) and an LMS-AE.

When  $A_L$  (8) is designed to be stable, which can be done similar to the design of  $\bar{A}$ , the state error system is stable. For the output  $\tilde{y}(k)$  of Subsystem 2, it can be expanded in the following form [19]

$$\begin{aligned} \tilde{y}(k) = & b_1 \tilde{y}(k-1) + b_2 \tilde{y}(k-2) + \cdots + b_{n_y} \tilde{y}(k-n_y) \\ & + v_0 d(k) + v_1 d(k-1) + \cdots + v_{n_d} d(k-n_d) \\ & - a_0 \hat{d}_e(k) - a_1 \hat{d}_e(k-1) - \cdots - a_{n_h} \hat{d}_e(k-n_h), \end{aligned} \quad (19)$$

where  $n_y$ ,  $n_d$ , and  $n_h$  are structural parameters, and  $b_1, \dots, b_{n_y}, v_0, \dots, v_{n_d}$ , and  $a_0, \dots, a_{n_h}$  are the coefficients.

**Theorem 2.** *If  $A_L$  is designed to be stable,  $a_0 = -\frac{\partial \tilde{y}}{\partial \hat{d}_e}(k) > 0$ , and the step size  $\mu$  satisfies*

$$0 < \mu < \min \left\{ \frac{2}{a_0 \sum_{i=0}^m d_{ni}^2(k)}, \frac{2}{\lambda_{max}^{d_n}} \right\} \quad (20)$$

*then the following statements hold.*

- 1) *Subsystem 2 is asymptotically stable for  $d(k) = 0$ .*
- 2) *The output error  $\tilde{y}(k)$  eventually converges to a bounded neighborhood for any bounded disturbance  $d(k)$ .*

*Proof.* Set a Lyapunov functional candidate as

$$V(k) = \frac{1}{2} \tilde{y}^2(k) \quad (21)$$

Define  $\Delta \tilde{y}(k) = \tilde{y}(k+1) - \tilde{y}(k)$ . Using Taylor series expansion, we have the following approximation:

$$\Delta \tilde{y}(k) \approx \sum_{i=0}^m \frac{\partial \tilde{y}}{\partial w_i}(k) \Delta w_i(k) + \frac{\partial \tilde{y}}{\partial d}(k) \Delta d(k). \quad (22)$$

where

$$\frac{\partial \tilde{y}}{\partial w_i}(k) = \frac{\partial \tilde{y}}{\partial \hat{d}_e}(k) \frac{\partial \hat{d}_e}{\partial w_i}(k) = -a_0 d_{ni}(k), \quad \frac{\partial \tilde{y}}{\partial d}(k) = v_0. \quad (23)$$

According to (14), we can obtain

$$\Delta w_i(k) = w_i(k+1) - w_i(k) = \mu d_{ni}(k) \tilde{y}(k). \quad (24)$$

Combining (22), (23), and (24),  $\Delta \tilde{y}(k)$  can be expressed as

$$\Delta \tilde{y}(k) = -\tilde{y}(k) h_1(k) + h_2(k) \quad (25)$$

where  $h_1(k) = \mu a_0 \sum_{i=0}^m [d_{ni}(k)]^2 > 0$  and  $h_2(k) = v_0 \Delta d(k)$ . Both of them are bounded for any time step  $k$  when  $d_{ni}$  are bound and Assumption 2 holds.

With (25), the difference of Lyapunuv candidate (21) becomes

$$\begin{aligned}\Delta V(k) &= \frac{1}{2} \Delta \tilde{y}(k) [2\tilde{y}(k) + \Delta \tilde{y}(k)] \\ &= [-\tilde{y}(k)h_1(k) + h_2(k)]\tilde{y}(k) + \frac{1}{2}[-\tilde{y}(k)h_1(k) + h_2(k)]^2 \\ &= -\tilde{y}^2(k)h_1(k)[1 - h_1(k)] + \tilde{y}(k)h_2(k)[1 - h_1(k)] + \frac{1}{2}h_2^2(k)\end{aligned}\quad (26)$$

For the case  $d(k) = 0$ ,  $h_2(k) = 0$ . The difference (26) of the Lyapunuv candidate reduces to  $\Delta V(k) = -\tilde{y}^2(k)[1 - \frac{1}{2}h_1(k)]$ , which is negative so long as  $\mu$  is selected by (20). By LaSalle invariance principle, the state converge to the hyperplane  $V(k) \equiv 0$ . Then,  $\tilde{y}(k) \equiv 0$  follows from (21). Therefore, Subsystem 2 is asymptotically stable.

For the case  $d(k) \neq 0$ , we see how the error  $\tilde{y}$  is bounded by the above stabilization process. It is easy to see that (26) is a convex quadratic function of  $\tilde{y}(k)$ . So, when solutions exists, we can obtain roots as

$$p_1(k) = \frac{h_2(k)}{h_1(k)}, \quad p_2(k) = \frac{h_2(k)}{h_1(k) - 2} \quad (27)$$

where they are both bounded for any  $k$ . According to (26), if  $\Delta V(k) < 0$ , the following condition must be satisfied

$$|\tilde{y}(k)| > \max_k \{|p_1(k)|, |p_2(k)|\} := \beta. \quad (28)$$

Obviously,  $\tilde{y}(k)$  will converge to the set  $\{\tilde{y}(k) : |\tilde{y}(k)| \leq \beta\}$ .

### 4.3 Inputs design for the LMS-AE

In the time domain, for a frequency component  $d_i(t) = A_i \sin(2\pi f_i t + \varphi_i)$  of the disturbance  $d(t)$

$$d_i(t) = A_i \cos(\varphi_i) \sin(\omega_i t) + A_i \sin(\varphi_i) \cos(\omega_i t). \quad (29)$$

The inputs of LMS-AE for  $f_i$  can be extended to following forms from  $d_{ni}$ :

$$d_{ni1}(t) = \sin(\omega_i t) = \sin(2\pi f_i t), \quad d_{ni2}(t) = \cos(\omega_i t) = \cos(2\pi f_i t). \quad (30)$$

On the other hand, by (10), in addition to the harmonic components, there may also be a DC component. So, it makes sense there is a constant input  $d_{n0} = 1$  to the LMS-AE. When the inputs of the LMS-AE are changed, then the asymptotic stability condition for Subsystem 2 is changed to

$$0 < \mu < \min \left\{ \frac{2}{a_0 \sum_{i=1}^m (d_{ni1}^2(k) + d_{ni2}^2(k)) + a_0}, \frac{2}{\lambda_{max}^{d_n}} \right\} \quad (31)$$

where the inputs  $d_n$  of the LMS-AE are also changed as  $d_n = [d_{n0}, d_{n11}, d_{n12} \cdots, d_{nm1}, d_{nm2}]^T$ .

*Design algorithm of LMS-AE-based control system:*

- Step 1* Select the appropriate  $(A_r, B_r)$  based on the reference inputs to the system.
- Step 2* Design suitable  $L$  and  $(K_p, K_r)$  that make  $A_L$  and  $\bar{A}$  stable, respectively.
- Step 3* When the absolute value of  $\tilde{y}(k)$  is greater than set threshold  $T_h$ ,  $\tilde{y}(k)$  sampled in period  $T_m$  is analyzed and the frequency characteristics of the disturbance is obtained.
- Step 4* Determine the filter inputs  $(d_{ni1}, d_{ni2})$  based on the information obtained in Step 3.
- Step 5* Choose a initial value for the weights  $w_i$  for the first time, and get a proper value of  $\mu$  for the estimator. Then start or continue iteration and adjust the weights by the updated law given in (31). Go to Step 3.

*Remark 2.* In Step 3, assume that the maximum period of disturbance is less than  $T_m$ , and  $T_h$  should be suitable.

## 5 Simulations and Analysis

In this section, a numerical example and a comparison with other method are used to validate the developed method.

In continuous-time domain, the state-space model of system is

$$A = \begin{bmatrix} 1 & 0 \\ -1 & -1 \end{bmatrix}, \quad B = \begin{bmatrix} 1 \\ 0 \end{bmatrix}, \quad C = [1 \ 0], \quad B_d = \begin{bmatrix} 1 \\ 1.2 \end{bmatrix}. \quad (32)$$

The reference input to the system is

$$r(t) = 20, \quad (0 \leq t \leq 35 \text{ s}), \quad (33)$$

and the disturbance  $d(t)$  is sum of two periodic disturbances:

$$d_1(t) = \begin{cases} 40(|t - 6.25| - 0.25), & (6 \text{ s} \leq t \leq 6.5 \text{ s}) \\ -40(|t - 6.75| - 0.25), & (6.5 \text{ s} \leq t \leq 7 \text{ s}) \\ d_1(t)(t - 1), & (7 \text{ s} \leq t \leq 20 \text{ s}) \end{cases} \quad (34)$$

$$d_2(t) = |10 \sin(4\pi t)| + 10 \sin(4\pi t), \quad (20 \text{ s} \leq t \leq 35 \text{ s}),$$

where the  $d_1(t)$  is a triangular wave of magnitude 10 with a frequency of 1.0 Hz.

Under sampling with  $T_s = 5 \text{ ms}$ , the discrete state-space model is

$$A = \begin{bmatrix} 1.000 & 0.005 \\ -0.005 & 0.995 \end{bmatrix}, \quad B = \begin{bmatrix} 0.005 \\ 0 \end{bmatrix}, \quad C = [1 \ 0], \quad B_d = \begin{bmatrix} 0.005 \\ 0.006 \end{bmatrix}. \quad (35)$$

According to (36), the proper  $(A_r, B_r)$  of the internal model are

$$A_r = 1, \quad B_r = 0.005. \quad (36)$$

Then, the suitable  $L$  and  $(K_p, K_r)$  are attained by discrete-time LQR method which make  $A_L$  and  $\bar{A}$  stable. The weight matrices of discrete-time LQR method are given as

$$Q_L = \text{diag}\{200, 200\}, R_L = 0.005, Q_K = \text{diag}\{20, 1, 20\}, R_K = 1, \quad (37)$$

which obtain

$$L = [0.6201 \ 0.2476]^T, K_p = [-5.1789 \ -0.8150], K_r = 4.4141. \quad (38)$$

And  $T_m$  and  $T_h$  are chosed as

$$T_h = 0.1, T_m = 3 \text{ s}. \quad (39)$$

**Table 1.** The frequencies of LMS-AE inputs over time tables.

Time	$f_1$	$f_2$	$f_3$	$f_4$	$f_5$	$f_6$
9-21 s	0.98 Hz	1.17 Hz	0.78 Hz	1.56 Hz	3.13 Hz	1.76 Hz
21-24 s	0.98 Hz	0.20 Hz	1.75 Hz	1.36 Hz	1.17 Hz	0.40 Hz
24-35 s	0.20 Hz	1.95 Hz	2.15 Hz	3.90 Hz	1.75 Hz	4.10 Hz

The simulation results in Fig. 4 denoted that the system was asymptotically stable, had superior disturbance rejection performance, and Table. 1 which denoted that the frequencies  $(f_1, f_2, \dots, f_6)$  of remaining filter inputs are updated by periodic time. Moreover, the system also had an excellent tracking performance due to the incorporation of the internal model. Although it took some time to acquire frequencies at the beginning of a new disturbance, this cannot hide its superior performance of disturbance rejection.

Finally, we compared the disturbance rejection performance of EID estimator with LMS-AE, and designed filter  $F(z)$  (40) for the EID estimator [8]

$$F(z) = \frac{0.2727z + 0.2727}{z - 0.4545}. \quad (40)$$

The simulation results in the Fig. 4 showed that disturbance rejection performance of LMS-AE was better than EID estimator.

## 6 Conclusion

An LMS-AE was designed to enhance the rejection performance of unknown periodic disturbances of control systems, which was based on the LMS algorithm and the EID concept. Then, the updated law and the convergence condition of weights for the LMS-AE were given. Moreover, by dividing the closed-loop system into two subsystems, stability conditions for the closed-loop system were obtained. Finally, the case study showed that the LMS-AE had superior performance.

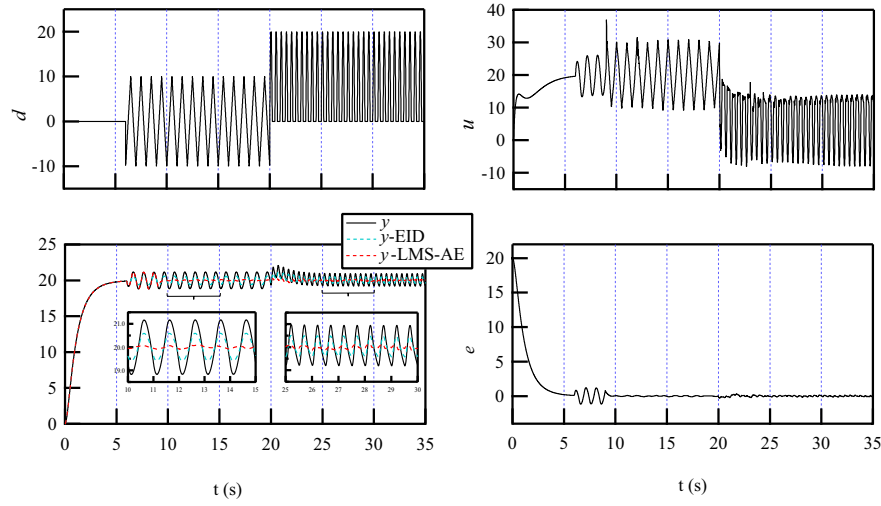


**Fig. 4.** Simulation results for LMS-AE-based and EID-based system with periodic disturbances.

## 7 ACKNOWLEDGMENTS

This work was supported by the National Natural Science Foundation of China under Grant 62003010 and by the R&D Program of Beijing Municipal Education Commission under Grant KM202410005036.

## References

1. T. Chowdhury et al.: Thermal management system for an electric machine with additively manufactured hollow conductors with integrated heat pipes. *IEEE Transactions on Industry Applications* 60(3), 3763-3772 (2024).
2. A. V. Vivas, A. Cherubini, M. Garabini, P. Salaris and A. Bicchi.: Minimizing energy consumption of elastic robots in repetitive tasks. *IEEE Transactions on Systems, Man, and Cybernetics: Systems* 53(8), 5006-5018 (2023).
3. K.-Z. Liu and Y. Yao.: *Robust control: theory and applications*. John Wiley & Sons (2016).
4. H. Muramatsu and S. Katsura.: An adaptive periodic-disturbance observer for periodic-disturbance suppression. *IEEE Transactions on Industrial Informatics* 14(10), 4446-4456 (2018).
5. K. Cho, J. Kim, S. B. Choi and S. Oh.: A high-precision motion control based on a periodic adaptive disturbance observer in a PMLSM. *IEEE/ASME Transactions on Mechatronics* 20(5), 2158-2171 (2015).
6. X. Feng, H. Muramatsu and S. Katsura.: Differential evolutionary algorithm with local search for the adaptive periodic-disturbance observer adjustment. *IEEE Transactions on Industrial Electronics* 68(12), 12504-12512 (2021).

7. L. Guo and W.-H. Chen.: Disturbance attenuation and rejection for systems with nonlinearity via DOBC approach. *International Journal of Robust and Nonlinear Control* 15(3), 109–125 (2005).
8. J. -H. She, M. Fang, Y. Ohyama, H. Hashimoto, and M. Wu.: Improving disturbance-rejection performance based on an equivalent-input-disturbance approach. *IEEE Transactions on Industrial Electronics* 55(1), 380–389 (2008).
9. J. She, K. Miyamoto, Q. -L. Han, M. Wu, H. Hashimoto, and Q. -G. Wang.: Generalized-extended-state-observer and equivalent-input-disturbance methods for active disturbance rejection: deep observation and comparison. *IEEE/CAA Journal of Automatica Sinica*, (2022).
10. J.-H. She, X. Xin, and Y. Pan.: Equivalent-input-disturbance approach-analysis and application to disturbance rejection in dual-stage feed drive control system. *IEEE/ASME Transactions on Mechatronics* 16(2), 330–340 (2011).
11. P. Yu, M. Wu, J. She, K.-Z. Liu, and Y. Nakanishi.: An improved equivalent-input-disturbance approach for repetitive control system with state delay and disturbance. *IEEE Transactions on Industrial Electronics* 65(1), 521–531 (2017).
12. L. Zhou, J. She, S. Zhou, and C. Li.: Compensation for state-dependent nonlinearity in a modified repetitive control system. *International Journal of Robust and Nonlinear Control* 28(1), 213–226 (2017).
13. J. R. Zeidler.: Performance analysis of LMS adaptive prediction filters. *Proceedings of the IEEE* 78(12), 1781–1806 (1990).
14. B. Widrow, J. M. McCool, M. G. Larimore, and C. R. Johnson.: Stationary and nonstationary learning characteristics of the LMS adaptive filter, *Proceedings of the IEEE* 64 (8), 1151–1162 (1976).
15. Y. Li, H.-L. Wei, and S. A. Billings.: Identification of time-varying systems using multi-wavelet basis functions. *IEEE Transactions on Control Systems Technology* 19(3), 656–663 (2011).
16. F. Wang and L. He.: FPGA-Based predictive speed control for PMSM system using integral sliding-mode disturbance observer. *IEEE Transactions on Industrial Electronics* 68(2), 972–981 (2021).
17. S. Haykin.: *Adaptive filter theory*. Englewood Cliffs, NJ: Prentice Hall, 1991.
18. P. Yu, K.-Z. Liu, J. She, M. Wu, and Y. Nakanishi.: Robust disturbance rejection for repetitive control systems with time-varying nonlinearities. *International Journal of Robust and Nonlinear Control* 29(5), 1597–1612 (2019).
19. Q. Liu, X. Huo, K. -Z. Liu and H. Zhao.: A parallelized input matching LMS adaptive filter for the rejection of spatially cyclic disturbances. *IEEE Transactions on Industrial Electronics* 70(10), 10536–10545 (2023).
20. M. Wu, B. Xu, W. Cao, and J. She.: Aperiodic disturbance rejection in repetitive-control systems. *IEEE Transactions on Control Systems Technology* 22(3) (2014).